ELSEVIER

Since January 2020 Elsevier has created a COVID-19 resource centre with free information in English and Mandarin on the novel coronavirus COVID-19. The COVID-19 resource centre is hosted on Elsevier Connect, the company's public news and information website.

Kappa-RBD produced by glycoengineered *Pichia pastoris* elicited high neutralizing antibody titers against pseudoviruses of SARS-CoV-2 variants

Taotao Mi [a,b], Tiantian Wang [b], Huifang Xu [b], Peng Sun [b], Xuchen Hou [b], Xinwei Zhang [b,c], Qian Ke [b,d], Jiawen Liu [b], Shengwei Hu [a,**], Jun Wu [b,***], Bo Liu [b,*]

[a] *College of Life Sciences, Shihezi University, Shihezi, Xinjiang, 832003, China*
[b] *Department of Microorganism Engineering, Beijing Institute of Biotechnology, Beijing, 100071, China*
[c] *College of Animal Science and Technology, Northwest A&F University, Yangling, Shaanxi, 712100, China*
[d] *Institute of Physical Science and Information Technology, Anhui University, Hefei, 230000, China*

ARTICLE INFO

ABSTRACT

The severe acute respiratory syndrome coronavirus 2 (SARS-CoV-2) kappa (B.1.617.1) variant represented the main variant of concern (VOC) for the epidemic in India in May 2021. We have previously established a technology platform for rapidly preparing SARS-CoV-2 receptor-binding domain (RBD) candidate vaccines based on glycoengineered *Pichia pastoris*. Our previous study revealed that the wild-type RBD (WT-RBD) formulated with aluminum hydroxide and CpG 2006 adjuvant effectively induces neutralizing antibodies in BALB/c mice. In the present study, a glycoengineered *P. pastoris* expression system was used to prepare recombinant kappa-RBD candidate vaccine. Kappa-RBD formulated with CpG and alum induced BALB/c mice to produce a potent antigen-specific antibody response and neutralizing antibody titers against pseudoviruses of SARS-CoV-2 kappa, delta, lambda, beta, and omicron variants and WT. Therefore, the recombinant kappa-RBD vaccine has sufficient potency to be a promising COVID-19 vaccine candidate.

1. Introduction

SARS-CoV-2 is responsible for the global COVID-19 pandemic. As of February 2022, more than 423 million cases of COVID-19 infections have been reported worldwide, with 5.8 million mortalities caused by COVID-19 infections (World Health Organization). SARS-CoV-2 infects the respiratory system with symptoms including cough and fever and acute respiratory distress in severe cases (Wang et al., 2020). The rapid spread of COVID-19, the severe clinical symptoms, and the emergence of virus variants require urgent development of new vaccines and treatments.

SARS-CoV-2 is an enveloped, single-stranded, positive-sense RNA virus (Li et al., 2020). The spike (S) glycoprotein, which induces neutralizing antibodies against viral infection, comprises a receptor-binding subunit S1 and a membrane fusion subunit S2. S is an essential part of the virus mechanism for binding, fusion, and entry into mammalian cells. The S1 subunit contains an *N*-terminal domain (NTD), a receptor-binding domain (RBD), and two small subdomains (Fig. 1a).

The RBD engages with the host cell receptor angiotensin-converting enzyme 2 (ACE2) (Lan et al., 2020; Xu et al., 2021; Hoffmann et al., 2020; Shang et al., 2020; Letko et al., 2020; Wrapp et al., 2020) for viral attachment to cells, whereas the S2 domain mediates cell-virus membrane fusion (Dai and Gao, 2021), facilitating the entry of the viral genome into host cells (Li, 2016). Viral entry is the initial and crucial step in the coronavirus infection cycle, and inhibiting RBD contact with ACE2 underpins immunological methods to prevent most coronavirus infections, including COVID-19. In addition, most neutralizing antibodies produced after SARS-CoV-2 infection or vaccines target the RBD (Dai and Gao, 2021; Baig et al., 2020). We showed previously that immunization of mice with the RBD of wild-type SARS-CoV-2 (WT-RBD) combined with aluminum hydroxide and CpG 2006 adjuvant triggered high titers of binding and neutralizing antibodies (Liu et al., 2021).

Since the outbreak of COVID-19, SARS-CoV-2 gene sequences containing various mutation sites have been deposited in the Global initiative on sharing all influenza data (GISAID). SARS-CoV-2 variants are characterized by the accumulation of evolutionary and genetic

---

a

b

WHO Label	Pango Lineage	RBD Mutant Sites
Beta	B.1.351	N501Y, E484K, K417N
Gamma	P.1	N501Y, E484K, K417T
Delta	B.1.617.2	T478K, L452R
Omicron	B.1.1.529	Y505H, N501Y, Q498R, G496S, Q493R, E484A, T478K, S477N, G446S, N440K, K417N, S375F, S373P, S371L, G339D
Lambda	C.37	F490S, L452Q

c

d

e

f
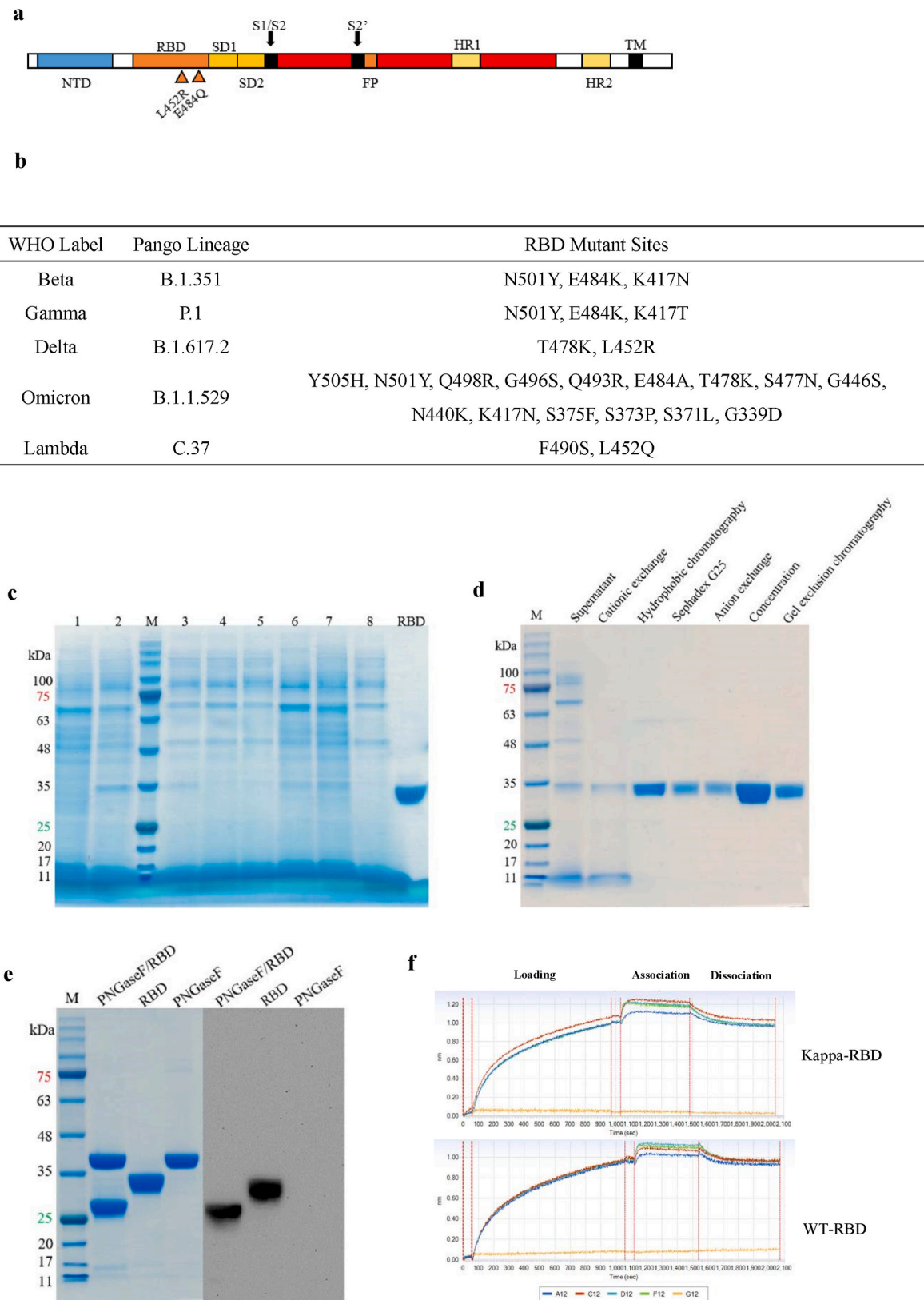
Fig. 1. SARS-CoV-2 receptor-binding domain (RBD) glycoprotein constructs. (a) Schematic of the S protein of SARS-CoV-2 kappa showing the position of the *N*-terminal domain (NTD), RBD, subdomains 1 and 2 (SD1 and SD2), fusion peptide (FP), heptad repeats 1 and 2 (HR1 and HR2), and transmembrane region (TM). (b) Mutations in the RBD of different SARS-CoV-2 variants. (c) SDS-PAGE analysis of various glycoengineered yeast/RBD clones. Each colony sample in Lanes 1-2-3-4-5-6-7-8. M: size markers; RBD: SARS-CoV-2 RBD. (d) SDS-PAGE analysis of the RBD purification process. (e) SDS-PAGE and western blotting results of RBD digested with PNGase F. (f) BLI profiles measuring the interaction between recombinant RBD and ACE2. A11, A12: 50 nM RBD; C11, C12: 100 nM RBD; D11, D12: 200 nM RBD; F11, F12: 400 nM RBD; G11, G12: baseline.

changes that cause greater infectivity and immune escape. Such changes may reduce the neutralization activity of current vaccines against these SARS-CoV-2 mutant strains. Recently, the SARS-CoV-2 variant kappa found in India has infected millions of people within a short period. Molecular characterization has revealed the presence of the non-synonymous substitutions G142D, E154K, L452R, E484Q, D614G, P681R, and Q1071H in this variant (Cherian et al., 2021). In the S protein, the L452R and E484Q substitutions are located in the RBD domain, and the L452R mutation increases infectivity and reduces the immune serum neutralizing activity of the virus considerably (Zhou et al., 2021a). Estimates of the levels of neutralizing activity in serum samples from vaccinated non-human primates and convalescent and mRNA-vaccinated populations have revealed that dual L452R and E484Q substitutions reduced the neutralizing activity of the antibodies (Li et al., 2021a).

In the present study, we designed a system to express a kappa mutant RBD vaccine in yeast and evaluated its effectiveness against SARS-CoV-2 pseudoviruses, facilitating the future development of SARS-CoV-2 preventive vaccines.

Ethics approval

All animal experiments were carried out according to the directive for the care and use of laboratory animals of the Institutional Animal Care and Use Committee of the Beijing Institute of Biotechnology and were approved by this committee. BALB/c mice were obtained from Beijing Vital River Laboratory Animal Technology Co., Ltd. All mice were raised in specific pathogen-free, individually ventilated cages and were given a standardized diet at the Animal Center of the Beijing Institute of Biotechnology. After each experiment, mice were asphyxiated by carbon dioxide and euthanized. The experimental animal welfare ethics number is IACUC-DWZX-2020-039.

2. Materials and methods

Cells, vectors, pseudoviruses, and antibodies. Trans1-T1 chemically competent cells were purchased from TransGen Biotech Co., Ltd (Beijing, China), and the pPICZαK vector and glycoengineered *Pichia pastoris* were prepared in our laboratory. 293T-ACE2 cells, pseudovirus SARS-CoV-2-Fluc lambda, beta, delta, kappa, omicron, and wild type (WT) were purchased from Vazyme Biotech Co., Ltd (Nanjing, China). Anti-SARS-CoV RBD antibody and horseradish peroxidase (HRP)-goat anti-rabbit immunoglobulin G (IgG) antibody were purchased from Sino Biological (Beijing, China). HRP-goat anti-mouse IgG (IgG1, IgG2a, IgG2b, and IgG3) antibodies were obtained from Abcam (Cambridge, MA, USA), and the monoclonal anti-polyhistidine-peroxidase antibody produced from mice was purchased from Sigma-Aldrich (St. Louis, MO, USA).

Plasmid construction and protein expression and purification. The kappa-RBD strain was constructed using the coding sequence of the WT SARS-CoV-2 strain (pPICZαA-RBD216) as the template. The RBD gene was cloned into the pPICZαK vector and transfected into glycoengineered *P. pastoris* by electroporation. The yeast, which cultured in the BMGY with a concentration of 1% methanol, expressed the target protein, as previously described (Liu et al., 2021).

The RBD was collected from the fermentation supernatant and purified successively by cation exchange (Capto MMC; GE Healthcare, USA), hydrophobic (Phenyl Sepharose low sub; GE Healthcare), strong anion exchange (Source 30Q; GE Healthcare), and gel exclusion chromatography (Superdex G75; GE Healthcare) chromatographies (Liu et al., 2021).

Protein structural assessment. The purified RBD was treated with peptide-N-asparagine (PNGase F), and the resulting protein was analyzed by SDS-PAGE and western blotting using anti-SARS-CoV spike S1 (rabbit) and HRP goat anti-rabbit IgG antibodies (dilution ratio of 1:2500).

The relative molecular mass, RBD reduction, and deglycosylation were analyzed by high-resolution XevoG2-XS QTOF [Waters (Shanghai) Co., Ltd.] mass spectrometry (MS). The liquid chromatography column (ACQUITY UPLC BEH300 C4, 1.7 μm, 2.1 × 50 mm) was equilibrated with solvent A [0.1% (v/v) formic acid (FA) (Fluka)], and the RBD was separated by different ratios of solvent A and solvent B (0.1% (v/v) FA in acetonitrile) and analyzed by XevoG2-XS QTOF MS.

The RBD purity was analyzed by high-performance liquid chromatography (HPLC) using a ZORBAX 300SB-C8 column (5 μm, 4.6 mm × 15 cm) (Agilent). The chromatographic column was equilibrated with 3% solvent B (0.1% (v/v) trifluoroacetic acid (TFA) in acetonitrile). After injecting the sample, gradient elution was carried out for 70 min (flow rate: 1.0 mL/min) (i.e., solvent A (0.1% (v/v) trifluoroacetic acid (TFA)) from 97% to 30%, solvent B from 3% to 70%). Recombinant RBD was then analyzed by size-exclusion chromatography using a TSKgel G3000sw HPLC column (5 μm, 4.6 mm × 25 cm) (TOSOH). After equilibrating this column with the mobile phase (0.1 M phosphate buffer, 0.1 M NaCl, pH 7), the sample was loaded onto the column and eluted over 30 min (flow rate: 0.5 mL/min).

Determination of the binding affinity of RBD to ACE2. Binding kinetic assays were performed by a Biolayer Interferometry (BLI) (ForteBIO® Octet QKe System) (Pall ForteBio Corporation, USA). First, the biosensor was washed for 1 min in HBS-EP buffer (0.01 M HEPES, 0.15 M NaCl, 3 mM EDTA, 0.005% (v/v) surfactant P20, pH 7.4). The biosensors were then loaded to saturation with His-ACE2 at 400 nM. Association was carried out over 400 s with serially diluted RBD (50, 100, 200, 400 nM). Finally, dissociation was also performed over 500 s. All proteins were diluted in HBS-EP buffer, and a loaded biosensor dipped in HBS-EP buffer served as the baseline. The results were analyzed using Octet Data Analysis Software (Pall ForteBio).

BALB/c mice immunization. Seven-week-old BALB/c female mice were randomized into five groups ($n = 10/14$). The mice were immunized with a hind shank-muscle injection (100 μL) of SARS-CoV-2 kappa-RBD (10 or 2.5 μg) with alum (100 μg) and CpG (50 μg) on days 0 and 14. Control mice were injected with RBD (10 μg) with aluminum hydroxide adjuvant (100 μg), aluminum hydroxide adjuvant (100 μg) plus CpG (50 μg), or normal saline (0.9% NaCl). Serum samples were collected before each injection and on day 28 and were preserved at −80 °C. In addition, the bodyweight of the mice was measured during immunization.

Serum from BALB/c mice was quantified for anti-RBD IgG by ELISA. Kappa-RBD (2 μg/mL) was coated on 96-well flat-bottom plates and incubated for about 10 h at 4 °C. Each well was washed twice with 1 × Phosphate Buffer Saline-Tween (PBST) and then sealed at 37 °C for 60 min with 300 μL of 5% (w/v) skim milk. The 5% (w/v) skim milk was discarded, and 100 μL of a gradient dilution of BALB/c mouse serum was added to wells. The plates were incubated for 60 min at 37 °C. Each plate was then washed with 1 × PBST five times, and 100 μL of the secondary antibody was added. The secondary antibodies, goat anti-mouse IgG-HRP (Sigma), IgG1-HRP, IgG2a-HRP, IgG2b-HRP, and IgG3-HRP (Abcam), were diluted 1:5000 and incubated for 60 min. Finally, the ELISA plate was washed with 1 × PBST five times, 3,3',5,5'-Tetramethylbenzidine (TMB) was added for color development for 5–8 min, and the reaction was terminated by adding 2 M sulfuric acid.

Enzyme-linked immunospot assay. Eight mice from the 10 μg RBD-Alum-CpG group and adjuvant groups were sacrificed seven days after the booster immunization, and the spleen was aseptically removed to prepare mice splenic cells. The splenic cells were counted and resuspended in Roswell Park Memorial Institute (RPMI) medium containing 10% (v/v) fetal bovine serum, 1% (w/v) penicillin/streptomycin, 1% (w/v) glutamine, and 55 μM 2-mercaptoethanol, and inoculated into precoated mouse ELISpot culture wells (Interferon-gamma (IFN-γ), interleukin-2 (IL-2) and Interleukin-4 (IL-4)) with 4×10^5 cells per well (two replicate wells). RPMI serum-free medium, recombinant RBD, CpG adjuvant, and concanavalin A were added to the wells. The final volume of each well was 0.2 mL. Coloration and imaging analysis was performed

after culturing for 20 h.

Pseudovirus neutralization assay. A pseudo neutralization test using antibody-mediated inhibition of the pseudovirus infection of 293T-ACE2 cells was performed on serum specimens using six commercially available SARS-CoV-2 pseudoviruses. First, serum samples were heated for 0.5 h at 56 °C to inactivate the complement. SARS-CoV-2-Fluc lambda, beta, delta, kappa, omicron, and wild type (WT) were incubated with continuously diluted serum samples at 37 °C for 60 min, and then the virus-antibody mixture (150 μL) was transferred to 96-well

plates precoated with 293T-ACE2 cells. Fresh medium was added 8 h later. After 48 h, 100 μL of the medium was discarded, and the luciferase assay substrate (100 μL) (Promega) was added. The plates were shaken for 2 min and incubated for 5 min at room temperature, and a multi-mode plate reader detected the fluorescence signal. GraphPad Prism 8 was used for nonlinear regression calculations to determine the half-maximal inhibitory concentration (IC_{50}) values.

Statistics. All statistical analyses and plotting were performed using SPSS 21.0, GraphPad Prism 8.0 software. A *t*-test was used between
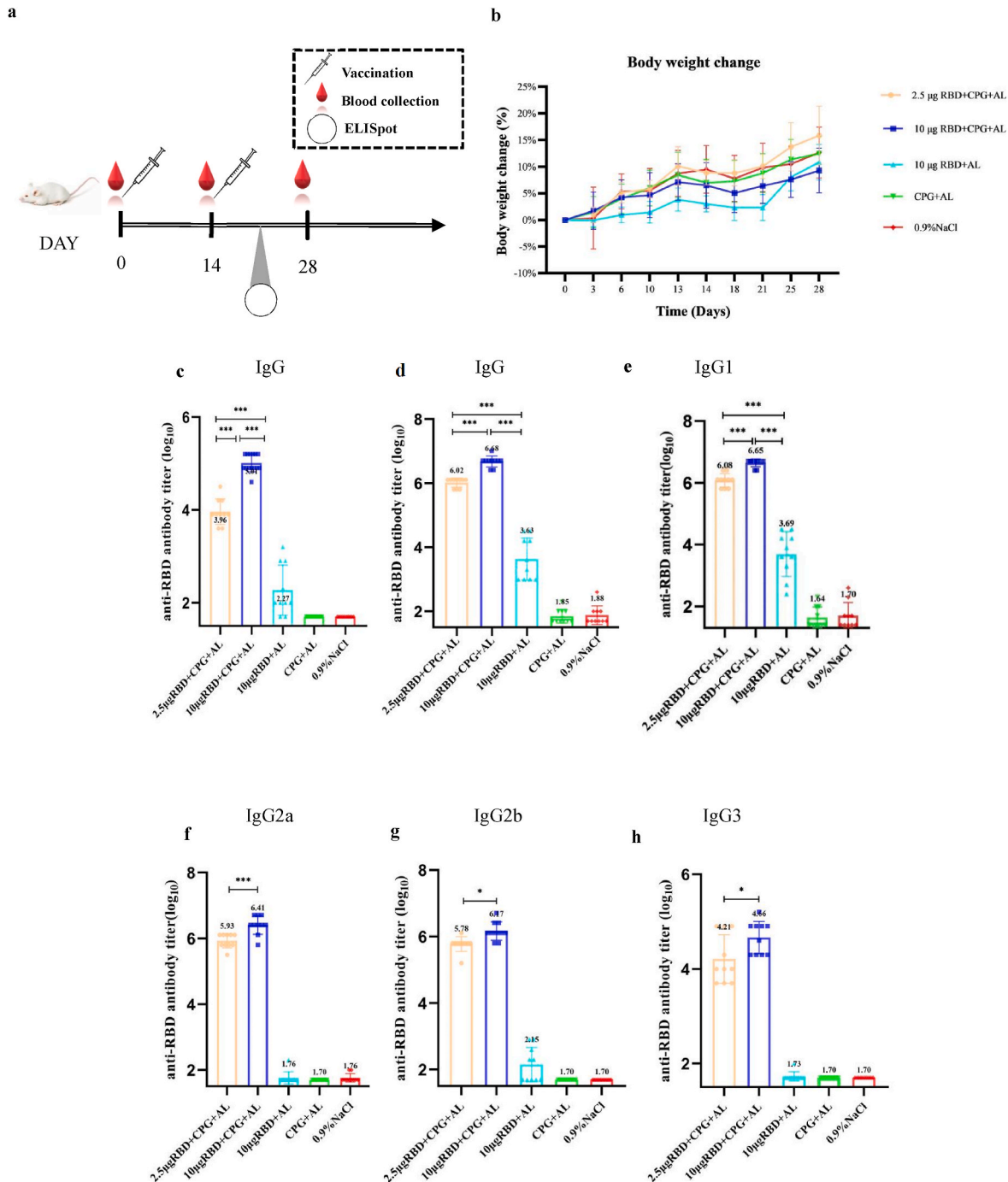
Fig. 2. Humoral immune responses to RBD vaccination by BALB/c mice. (a) Immunological strategy for BALB/c mice. (b) Changes in the bodyweight of mice from different test and control groups. (c) Antibody titers after initial immunization with vaccines containing different adjuvant components and different antigen doses. (d) Antibody titers after the second immunization with vaccines containing different adjuvant components and different antigen doses. Specific (e) IgG1, (f) IgG2a, (g) IgG2b, and (h) IgG3 antibody titers after the second immunization with vaccines containing different adjuvant components and different antigen doses. The *P*-values were determined by an independent *t*-test (*$P < 0.05$, **$P < 0.01$, ***$P < 0.005$). Normal saline: 0.9% (w/v) NaCl.

groups, and *P < 0.05* was considered significant (*P < 0.05, **P < 0.01, ***P < 0.005*).

3. Results

RBD was prepared by eukaryotic expression and purification. The SARS-CoV-2 kappa RBD gene encodes a glycoprotein (amino acids 319–534 of the S protein) 216 amino acids in length with E484Q, and L452R mutations (Fig. 1a). Mutations in the SARS-CoV-2 RBD for each variant are listed in Fig. 1b.

The RBD was expressed in a glycoengineered *P. pastoris* expression system (Fig. 1c). The proteins expressed in yeast were purified by cationic exchange, hydrophobic, anion exchange, and gel exclusion chromatographies (Fig. 1d) (Liu et al., 2021). The purified RBD was verified by SDS-PAGE and western blotting with a molecular weight <35 kDa (Fig. 1e).

High-resolution XevoG2-XS Q-TOF MS revealed that the recombinant RBD has a molecular weight of 26985.00 Da and the molecular weight of the deglycosylated RBD is 23732.75 Da (Fig. S1).

After SEC-HPLC (TSKgel G3000sw, TOSOH) and RP-HPLC (Agilent, ZORBAX 300SB-C8) analysis, the RBD sample yielded a single peak (Fig. S2), indicating a protein purity of 100%.

The affinity of kappa-RBD and WT-RBD toward the His-ACE2 ectodomain was determined by BLI (Fig. 1f and Table S1). The results showed that the affinity of His-ACE2 for Kappa-RBD ($K_D = 25.65$ nM) is ~1.87-fold higher than that measured for WT-RBD ($K_D = 48.03$ nM).

RBD vaccine-induced humoral immunity. The bodyweight of the mice in each group increased following immunization (Fig. 2b). The immunogenicity of the RBD was validated by evaluating the humoral immune response of immunized and control BALB/c mice. Two weeks after the first immunization, the BALB/c mice serum titer in the 10 μg RBD-Alum-CpG group was 1.11×10^5, the serum titer of mice in the 2.5 μg RBD-Alum-CpG group was 1.12×10^4, and the serum antibody titer of mice in the 10 μg RBD-Alum group was 3.9×10^2. A significant difference between the three groups was observed (*P < 0.001*). Two weeks after the booster immunization, the serum antibody titer of the mice in the 10 μg RBD-Alum-CpG group was 5.12×10^6, the serum antibody titer of the mice in the 2.5 μg RBD-Alum-CpG group was 1.08×10^6, and the serum antibody titer of the mice in the 10 μg RBD-Alum group was 1.06×10^4, and the difference in the antibody titers between the three groups was highly significant (*P < 0.001*) (Fig. 2c–e). The results showed that the 10 μg RBD dose induced higher total anti-RBD IgG titers, indicating that a higher antigen dose increased the levels of antibodies.

The ratio of IGg1/IGg2a reflects the dominant response type in the body, and IgG2 can interact with FcRI, FcRII, FcRIII, and FcRIIV (Beers et al., 2016). Thus, IgG2a antibodies should be more effective than IgG1 antibodies in clearing viral infections. The present study analyzed the titers of different IgG-type antibodies, IgG1, IgG2a, IgG2b, and IgG3, in the serum after immunization with the RBD vaccine. The results showed that the 10 μg RBD-Alum-CpG group had a high titer of IgG1, IgG2a, IgG2b, and IgG3 (Fig. 2f–h). High titers of IgG2a from the 10 μg RBD-Alum-CpG group indicate an immune-induced T helper cell 1 (Th1)-biased response, which may provide improved protection against novel coronavirus infections when compared with that of the Alum-CpG group. The 10 μg RBD-Alum group had a low antibody titer, except for the IgG1 isoform. Aluminum hydroxide gel often yields a Th2-type response, producing more IgG1. After CpG was added, the Th1-type response and the antibody titers of all isoforms increased. Thus, different adjuvants can transform the type of isoforms of the antigen-specific antibodies from IgG1 to IgG2, which expands the vaccine protection profile.

The RBD vaccine induced a cellular immune response. Interleukin-4 (IL-4) facilitates the differentiation of Th0 cells into Th2 cells, which can continuously secrete Th2-type cytokines IL-4 and interleukin-5 (IL-5). IL-4 promotes the conversion of antibodies to IgG1. Interferon-gamma

(IFN-γ) and interleukin-2 (IL-2) promote the differentiation of Th0 to Th1, and Th1 cells can continue to secrete IFN-γ and IL-2. To examine the antigen-specific T cell response, we isolated splenocytes one week after the booster immunization to detect the response of the cytokines IFN-γ, IL-2, and IL-4 toward the RBD and CpG. Compared with the Alum-CpG group, in the 10 μg RBD-Alum-CpG group, stimulation with the RBD caused significant increases in the levels of IFN-γ, IL-2, and IL-4 (121–206 spots/4×10^5 cells, 114–203 spots/4×10^5 cells, and 85–157 spots/4×10^5 cells, respectively) (Fig. 3a). In addition, compared with the 10 μg RBD-Alum-CpG group, the secretion of IFN-γ, IL-2, and IL-4 in the Alum-CpG group under CpG stimulation was increased significantly (142–215 spots/4×10^5 cells, 19–91 spots/4×10^5 cells, and 6–32 spots/4×10^5 cells, respectively) (Fig. 3b). Therefore, the 10 μg RBD-Alum-CpG group produced a Th1-biased response, and CpG promotes this biased response to prevent viral infection.

Pseudovirus-neutralizing activity. We evaluated the neutralizing antibody titers using several pseudovirus assays of serum samples isolated from mice (10 μg RBD-Alum-CpG group) two weeks after the booster vaccination. Compared with the neutralizing antibody titer against the kappa pseudovirus, the neutralizing antibody titer against the delta variant decreased by 3.78-fold, the neutralization titer against the lambda variant increased by 12.14-fold, and the neutralization titer against the beta variant increased by 2.22-fold (Fig. 4a). These results indicated that the designed vaccine produced broad-spectrum antibodies against several variants.

The Omicron variant of SARS-CoV-2 with the largest number of mutations was first confirmed on November 9, 2021, and WHO cautioned that the Omicron variant held a very high risk of infection. We need COVID-19 vaccines that can effectively resist new strains. The immune serum of our kappa-RBD vaccine can be used against the pseudovirus of Omicron and WT with IC_{50} values of 2.606 and 2.334, respectively (Fig. 5).

4. Discussion

Since the outbreak of the COVID-19 pandemic, continuously emerging novel mutants have caused infections with increased severity or reduced the effectiveness of currently used vaccines. Therefore, it is desirable to develop safer and more effective vaccines. Similar to the other five SARS-CoV-2 variant (alpha, beta, gamma, delta, and omicron) (World Health Organization; Garcia-Beltran et al., 2021; Zhou et al., 2021b; Supasa et al., 2021), the kappa variant was the main VOC that caused the epidemic in India in May 2021. In contrast with the currently approved or authorized COVID-19 vaccines (inactivated, adenovirus vector, and mRNA vaccines) (World Health Organization), recombinant protein vaccines show better uniformity and higher safety. The RBD of the S protein prepared by insect cells and the Bac-to-Bac baculovirus expression system has been shown to have good immunogenicity, and immune serum from mice or rabbits can neutralize pseudoviruses and vaccine protected primates (*M. mulatta*) from SARS-CoV-2 (Yang et al., 2020). Moreover, our previous study has established a technology platform in our laboratory for preparing RBD candidate vaccines rapidly based on *Pichia pastoris*. Yeast expression systems have the merits of high expression efficiency and low cost but have the disadvantage of excessive mannose modification of glycoproteins. Glycosylation engineering in yeast has solved this problem (Choi et al., 2003; Li et al., 2006; Callewaert et al., 2001). Our laboratory has demonstrated previously that transformed glycosylation engineering in *P. pastoris* can ensure correct glycosylation modifications without masking the RBD epitopes (Li et al., 2021a). In the present study, SARS-CoV-2 kappa-RBD was expressed by the glycoengineered *P. pastoris* expression system, and the immune response to the vaccine was comprehensively evaluated.

The RBD molecular weight detected by high-resolution XevoG2-XSQ-TOF MS was inconsistent with the molecular weight of the deglycosylated protein because there are two glycosylation sites in the protein.

Compared with the WT RBD, amino acid exchanges for different
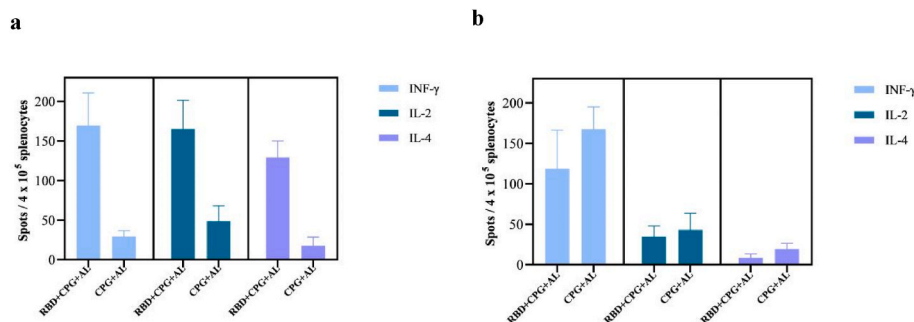
Fig. 3. Cellular immune responses by BALB/c mice to vaccination with 10 μg RBD. (a) Splenic IFN-γ, IL-2, and IL-4 ELIspot responses to the SARS-CoV-2 RBD antigen. (b) Splenic IFN-γ, IL-2, and IL-4 ELIspot responses to CpG. SFCs: Spot-forming cells.
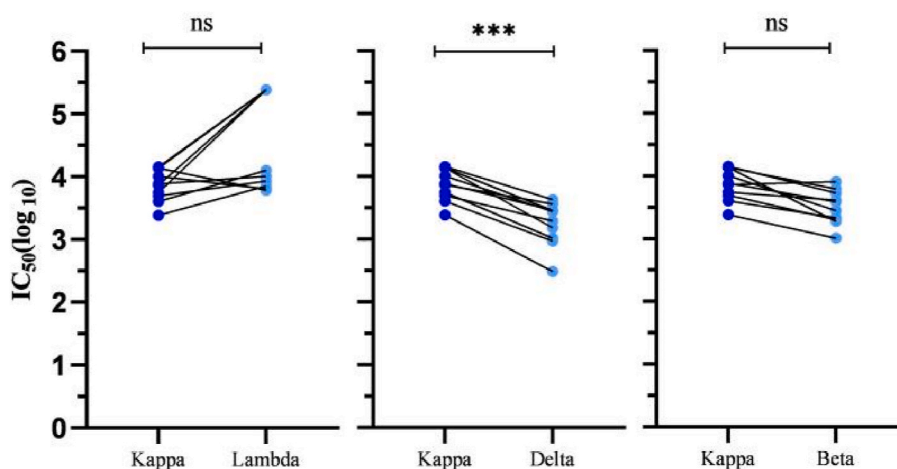
Fig. 4. Neutralizing activity against the pseudoviruses (SARS-CoV-2 kappa, lambda, delta, and beta) following vaccination with RBD. The *P*-values were determined by an independent *t*-test (*$P < 0.05$, **$P < 0.01$, ***$P < 0.005$). IC$_{50}$: half maximal inhibitory concentration.

mutants are L452Q and F490S for lambda RBD, L452R and E484Q for kappa RBD, K417N, E484K, and N501Y for beta RBD, L452R and T478K for delta RBD, and Y505H, N501Y, Q498R, G496S, Q493R, E484A, T478K, S477N, G446S, N440K, K417 N, S375F, S373P, S371L, and G339D for omicron RBD. Studies have shown that the L452R substitution increases infectivity, but this variant has weak binding to immune serum (Baig et al., 2020). However, when both L452R and E484Q substitutions are present, the infectivity increases significantly, and the binding affinity to immune serum is weak (Liu et al., 2021). The N501Y mutation may be associated with transmissibility and increased binding affinity toward ACE2 (Ali et al., 2021; Leung et al., 2021). The E484K mutation infers antibody resistance (Li et al., 2021b), whereas the L452Q, T478K, and F490S substitutions have been found to enhance immune escape capability (Kimura et al., 2021; Wilhelm et al., 2021). The K417N, E484K, and N501Y mutations increase the binding affinity toward ACE2 and ultimately increase infectivity (Abbas et al., 2021). Many mutations in the RBD of the S protein from the omicron variant are responsible for the higher affinity toward ACE2 (Wang and Cheng, 2022; Kumar et al., 2022). In our study, compared with the neutralization activity of the immune serum toward the RBD (L452R and E484Q), the neutralization activity toward the RBD (L452R and T478K) decreased, and the neutralization activity toward the RBD (L452Q and F490S) and RBD (K417N, E484K, and N501Y) increased. The high binding antibody titer and neutralization activity showed that the vaccine had good immunogenicity in BALB/c mice and had broad-spectrum protection against mutant strains, which has the potential to strengthen immunization. We further demonstrated that the vaccine had a protective effect against strains containing L452Q, F490S, L452R, E484Q, K417N, E484K, and N501Y mutations and had a weak protective effect against

strains containing the T478K substitution. Although the omicron variant has many mutations, our vaccine displayed potential protection against this variant.

Recombinant proteins generally cause only a weak immune response. Most vaccines are mixed with adjuvants to enhance the immune response and ensure specific antigen doses. The US Food and Drug Administration (FDA) has clearly stated in industry guidelines that, in addition to inducing a high titer of neutralizing antibodies (A and Development and Lice, 2020), vaccines should induce a strong Th1-tilted CD4 T cell response. Several studies have shown that candidate SARS-CoV-2 vaccines prepared with an aluminum hydroxide gel can induce a specific Th2-biased response and may induce pulmonary eosinophilic immunopathology in murine models (Honda-Okubo et al., 2015). Therefore, most COVID-19 recombinant protein vaccine formulations with aluminum hydroxide gel include a second adjuvant, such as CpG, to balance the immune response and stimulate the proliferation of Th1-type CD4(+) cells. In the present study, through IgG typing of specific antibodies and cytokines, we demonstrated that a vaccine containing aluminum and CpG adjuvants triggers a Th1-biased response; thus, providing better protection against the virus. Noteworthy, the kappa-RBD formulated vaccine with CpG and alum induced pseudovirus neutralizing antibody titers against SARS-CoV-2 kappa, delta, lambda, beta, and omicron variants as well as the WT virus. These results indicate that the designed vaccine has broad-spectrum activity and the potential to inhibit mutant strains that may appear in the future.

Availability of data and material

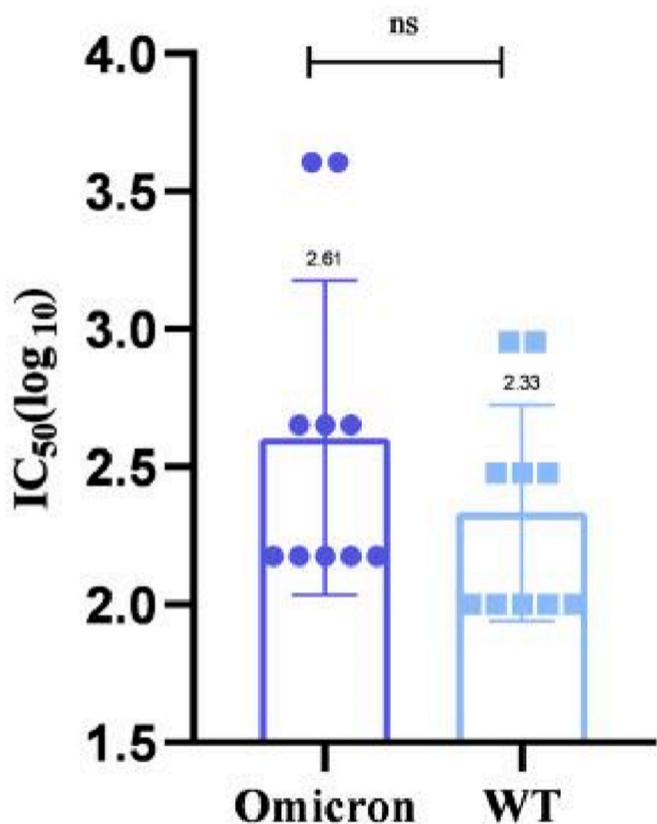The data used to support the conclusions of this study are presented

Fig. 5. Neutralization by immune serum against pseudoviruses of omicron and wild-type (WT) SARS-CoV-2. The *P*-values were determined by an independent *t*-test (*$*P < 0.05$, $**P < 0.01$, $***P < 0.005$*). IC_{50}: half maximal inhibitory concentration.

in the text and supplementary materials.

Consent to participate

All authors reviewed and approved the manuscript.

CRediT authorship contribution statement

Taotao Mi: carried out the experiments, Formal analysis, Writing – original draft, Writing – review & editing. **Tiantian Wang:** carried out the experiments, Formal analysis. **Huifang Xu:** carried out the experiments, Formal analysis. **Peng Sun:** carried out the experiments, Formal analysis. **Xuchen Hou:** carried out the experiments, Formal analysis. **Xinwei Zhang:** Writing – review & editing. **Qian Ke:** carried out the experiments, Formal analysis. **Jiawen Liu:** Writing – review & editing. **Shengwei Hu:** Supervision. **Jun Wu:** Conceptualization, Resources, Supervision. **Bo Liu:** Conceptualization, Resources, Supervision.

Declaration of competing interest

The authors declare that they have no known competing financial interests or personal relationships that could have appeared to influence the work reported in this paper.

Acknowledgments

Appendix A. Supplementary data

Supplementary data to this article can be found online at https://doi.org/10.1016/j.virol.2022.03.001.

References

FDA, 2020. Development and Licensure of Vaccines to Prevent COVID-19. Guidance for Industry.

Abbas, K., Tauqir, Z., Muhammad, S., et al., 2021. Higher infectivity of the SARS-CoV-2 new variants is associated with K417N/T, E484K, and N501Y mutants: an insight from structural data [J]. J. Cell. Physiol. 1–13.

Ali, F., Kasry, A., Amin, M., 2021. The new SARS-CoV-2 strain shows a stronger binding affinity to ACE2 due to N501Y mutant [J]. Med. Drug Discov. 10, 100086.

Baig, A.M., Khaleeq, A., Syeda, H., 2020. Elucidation of cellular targets and exploitation of the receptor-binding domain of SARS-CoV-2 for vaccine and monoclonal antibody synThesis [J]. J. Med. Virol. 92, 2792–2803.

Beers, S.A., Glennie, M.J., White, A.L., 2016. Influence of immunoglobulin isotype on therapeutic antibody function [J]. Blood 127, 1097–1101.

Callewaert, N., Laroy, W., Cadirgi, H., et al., 2001. Use of HDEL-tagged Trichoderma reesei mannosyl oligosaccharide 1,2-α-D-mannosidase for N-glycan engineering in *Pichia pastoris* [J]. FEBS Lett. 503 (2–3), 173–178.

Cherian, S., Potdar, V., Jadhav, S., et al., 2021. Convergent evolution of SARS-CoV-2 spike mutations, L452R, E484Q and P681R. In: The Second Wave of COVID-19 in Maharashtra, India [J]. bioRxiv Preprint, 9, p. 1542, 7.

Choi, B.K., Bobrowicz, P., Davidson, R.C., et al., 2003. Use of combinatorial genetic libraries to humanize N-linked glycosylation in the yeast *Pichia pastoris* [J]. Proc. Natl. Acad. Sci. U.S.A. 100 (9), 5022–5027.

Dai, L., Gao, G.F., 2021. Viral targets for vaccines against COVID-19 [J]. Nat. Rev. Immunol. 21, 73–82.

Garcia-Beltran, W.F., Lam, E.C., Denis, StK., et al., 2021. Multiple SARS-CoV-2 variants escape neutralization by vaccineinduced humoral immunity [J]. Cell 184 (9), 2372–2383 e9.

Hoffmann, M., Kleine-Weber, H., Schroeder, S., et al., 2020. SARS-CoV-2 cell entry depends on ACE2 and TMPRSS2 and is blocked by a clinically proven protease inhibitor[J]. Cell 181 (2), 271–280 e278.

Honda-Okubo, Y., Barnard, D., Ong, C.H., et al., 2015. Severe acute respiratory syndrome-associated coronavirus vaccines formulated with delta inulin adjuvants provide enhanced protection while ameliorating lung eosinophilic immunopathology [J]. Virol 89, 2995–3007.

Kimura, I., Kosugi, Y., Wu, J.Q., et al., 2021. SARS-CoV-2 Lambda variant exhibits higher infectivity and immune resistance. [J]. bioRxiv. 28, 454085, 07.

Kumar, S., Thambiraja, T.S., Karuppanan, K., et al., 2022. Omicron and Delta variant of SARS-CoV-2: a comparative computational study of spike protein [J]. J. Med. Virol. 94 (4), 1641–1649.

Lan, J., Ge, J., Yu, J., et al., 2020. Structure of the SARS-CoV-2 spike receptor-binding dom ain bound to the ACE2 receptor [J]. Nature 581, 215–220.

Letko, M., Marzi, A., Munster, V., 2020. Functional assessment of cell entry and receptor usage for SARS-CoV-2 and other lineage B betacoronaviruses [J]. Nat.Microbiol. 5, 562–569.

Leung, K., Shum, M.H., Leung, G.M., et al., 2021. Early transmissibility assessment of the N501Y mutant strains of SARS-CoV-2 in the United Kingdom, October to November 2020 [J]. Euro Surveill. 26, 2002106.

Li, F., 2016. Structure, function, and evolution of coronavirus spike proteins [J]. Annual Review of Virology 3 (1), 237–261.

Li, H., Sethuraman, N., Stadheim, T.A., et al., 2006. Optimization of humanized IgGs in glycoengineered *Pichia pastoris* [J]. Nat. Biotechnol. 24 (2), 210–215.

Li, T.T., Zheng, Q.B., Yu, H., et al., 2020. SARS-CoV-2 spike produced in insect cells elicits high neutralization titres in non-human primates [J]. Emerg. Microb. Infect. 9 (1), 2076–2090.

Li, G., Zhou, Z.C., Du, P., et al., 2021a. The SARS-CoV-2 spike L452R-E484Q variant in the Indian B.1.617 strain showed significant reduction in the neutralization activity of immune sera [J]. Precision Clin. Med. 1–6, 0(0).

Li, Q., Nie, J., Wu, J., et al., 2021b. SARS-CoV-2 501Y.V2 variants lack higher infectivity but do have immune escape [J]. Cell 184, 2362–2371 e9.

Liu, B., Yin, Y., Liu, Y.X., et al., 2021. A vaccine based on the receptor-binding domain of the spike protein expressed in glycoengineered Pichia pastoris targeting SARS-CoV-2 stimulates neutralizing and protective antibody responses. J. Eng. 7.

Shang, J., Ye, G., Shi, K., et al., 2020. Structural basis of receptor recognition by SARS-CoV-2 [J]. Nature 581 (7807), 221–224.

Supasa, P., Zhou, D., Dejnirattisai, W., et al., 2021. Reduced neutralization of SARS-CoV-2 B.1.1.7 variant by convalescent and vaccine sera [J]. Cell 184 (8), 2201–2211 e7.

Wang, L., Cheng, G., 2022. Sequence analysis of the emerging SARS-CoV-2 variant omicron in South Africa [J]. J. Med. Virol. 94 (4), 1728–1733.

Wang, D., Hu, B., Hu, C., et al., 2020. Clinical characteristics of 138 hospitalized patients with 2019 novel coronavirus -infected pneumonia in Wuhan, China [J]. JAMA 11, 1061–1069.

Wilhelm, A., Toptan, T., Pallas, C., et al., 2021. Antibody-mediated neutralization of authentic SARS-CoV-2 B.1.617 variants harboring L452R and T478K/E484Q [J]. Viruses 13, 1693.

World Health Organization. WEekly Operational Update on Coronavirus Disease (COVID-19).

Wrapp, D., Wang, N., Corbett, K.S., et al., 2020. Cryo-EM structure of the 2019-nCoV spikein the prefusion conformation [J]. Science 367, 1260–1263.

Xu, C., Wang, Y., Liu, C., et al., 2021. Conformational dynamics of SARS-CoV-2 trimeric spike glycoprotein in complex with receptor ACE2 revealed by cryo-EM [J]. Sci. Adv. 7.

Yang, J., Wang, W., Chen, Z., et al., 2020. A vaccine targeting the RBD of the S protein of SARS-CoV-2 induces protective immunity [J]. Nature 586, 572–577.

Zhou, Z.C., Du, P., Yu, M.X., et al., 2021a. Assessment of infectivity and the impact on neutralizing activity of immune sera of the COVID-19 variant, CAL.20C [J]. Signal Transduct. Target Ther. 6 (1), 285.

Zhou, D., Dejnirattisai, W., Supasa, P., et al., 2021b. Evidence of escape of SARS-CoV-2 variant B.1.351 from natural and vaccine-induced sera [J]. Cell 184 (9), 2348–2361 e6.